AEM Accepted Manuscript Posted Online 18 May 2018
Appl. Environ. Microbiol. doi:10.1128/AEM.00830-18

Modifying the lantibiotic mutacin 1140 for increased yield, activity and stability

Mengxin Geng,[a] and Leif Smith[a]

[a]Department of Biology, College of Science, Texas A&M University, College Station, Texas, USA

Corresponding Author

***** Tel (L. Smith): 979-845-2417, Fax: 979-845-2891, Email: jsmith@bio.tamu.edu

Present Address

‖Department of Biology, Texas A&M University, College Station, TX 77843,

ABSTRACT

Mutacin 1140 belongs to the epidermin family of type AI lantibiotics. This family has a broad spectrum of activity against Gram-positive bacteria. The binding of mutacin 1140 to lipid II leads to the inhibition of cell wall synthesis. Pharmacokinetic experiments on type AI lantibiotics are generally discouraging for clinical applications due to their short half-life. The unprotected dehydrated and protease susceptible residues outside of the lanthionine rings may play a role in their short half-life in physiological settings. Previous mutagenesis work on mutacin 1140 has been limited to the lanthionine-forming residues, C-terminal decarboxylated residue, and single amino acid substitutions in positions Phe1, Trp4, Dha5, and Arg13. To study the importance of the dehydrated (Dha5 and Dhb14) and protease susceptible (Lys2 and Arg13) residues within mutacin 1140 for stability and bioactivity, each of these residues were evaluated for their impact on production and inhibitory activity. More than 15 analogs were purified, enabling the direct comparison of the activity against a select panel of Gram-positive bacteria. The efficiency of the post-translational modification (PTM) machinery of mutacin 1140 is highly restricted on its substrate. Analogs in the various intermediate stages of PTMs were observed as minor products following single point mutations at 2^{nd}, 5^{th}, 13^{th}, and 14^{th} positions. The combination of alanine substitutions at the Dha5 and Dhb14 positions abolished mutacin 1140 production, while the production was restored with the substitutions of a Gly residue at one of these positions. Analogs with improved activity, productivity and proteolytic stability were identified.

IMPORTANCE

Our findings show that the efficiency of the mutacin 1140 PTMs is highly dependent on the core peptide sequence. Analogs in various intermediate stages of PTMs can be transported by the bacterium, which indicates that PTMs and transport are finely tuned for the native mutacin 1140 core peptide. Only certain combinations of amino acid substitutions at the Dha5 and Dhb14 dehydrated residue positions were tolerated. Observation of glutamylated core peptide analogs show that dehydrations occur in a glutamate dependent manner. Interestingly, mutations in positions outside of rings A and B, the lipid II binding domain, would interfere with lipid II binding. Purified mutacin 1140 analogs have varying activity and selectivity against different genera of bacteria, supporting the effort to generate analogs with higher specificity against pathogenic bacteria. The discovery of analogs with improved inhibitory activity against pathogenic bacteria, increased protease stability, and higher product yields, may promote the clinical development of this unique antimicrobial compound.

INTRODUCTION

Lanthipeptides are a class of lanthionine-containing, ribosomally synthesized and post-translationally modified peptides (RiPPs), and lanthipeptides with antimicrobial activities are termed as lantibiotics (1). Lanthionine (Lan) or methyllanthionine (MeLan) rings are formed by a thioether linkage between a cysteine residue and a dehydrated 2,3-didehydroalanine (Dha) or 2,3-didehydrobutyrine (Dhb) residue, respectively (2). The Dha

and Dhb residues are derived from the dehydration of a serine and threonine, respectively. The biosynthetic gene cluster for type AI lantibiotics contains genes that encode the lantibiotic peptide *lanA*, the dehydratase *lanB* (3-5), the cyclase *lanC* (3, 6), and the transporter *lanT* (7). The mutacin 1140 operon also contains an additional gene *lanD*, which encodes a flavoprotein that is responsible for the C-terminal decarboxylation of the core peptide forming an aminovinyl-cysteine (AviCys) residue (8). The dehydratase of nisin functions through a tRNA-dependent manner (Figure 1A). The alcohol of the serine or threonine residues are glutamylated with the help of $tRNA^{Glu}$, and subsequently the glutamate is eliminated to generate the dehydrated residue Dha or Dhb (5, 9). Nisin autoregulates its own biosynthesis by binding to the transmembrane kinase NisK. The kinase phosphorylates its intracellular response regulator NisR and is followed by activation of the *nis* promoter and translation of the *nis* operon (10). However, *mutR* is the first gene in the mutacin 1140 biosynthetic gene cluster (11). There is no report confirming the autoregulation of mutacin 1140 biosynthesis and genes corresponding to *nisK* have not yet been identified. It has been suggested that additional uncharacterized regulatory elements other than MutR may play a major role in the production and regulation of mutacin I and II (1214), while little is known about the production and regulation of mutacin 1140.

Type AI lantibiotics, including the nisin and epidermin family (Figure 1B), generally possess a broad spectrum of activity against Gram-positive bacteria. Their conserved N-terminal rings A and B represent the lipid II binding motif (Figure 1C), which targets the pyrophosphate, peptidoglycan MurNAc, and the first isoprene of cell wall precursor lipid II (15-18). The complex formed between nisin or mutacin 1140 with lipid II is extremely tight:

79 mutacin or nisin could not competitively compete against each other for lipid II once the
80 lantibiotic/lipid II complex was formed (19). However, apart from the N-terminal rings, there
81 is little structural similarity between the two peptides. The C-terminal residue of mutacin
82 1140 is decarboxylated and is involved in lanthionine ring D formation, while the C-terminal
83 residues of nisin retains its carboxyl group. C-terminal domain of nisin is much longer than
84 mutacin, which is believed to be responsible for pore formation activity of nisin (20). Nisin
85 forms large transmembrane pores on giant unilamellar vesicles (GUVs), while mutacin 1140
86 does not (17). Furthermore, mutacin 1140 was not able to permeabilize the cytoplasmic
87 membrane of a sensitive strain of *Streptococcus rattus* (19). The lantibiotics epidermin and
88 gallidermin differ from mutacin 1140 primarily in amino acid composition at the N-terminal
89 and ring A region of the core peptide, but the peptide backbone length of ring A does not
90 change. Epidermin was shown to form pores in phosphatidylcholine/cholesterol liposomes
91 with the addition of 0.1 mol lipid II, but it was not clear if epidermin could promote leakage
92 of susceptible bacterial cells (15). Gallidermin did not form pores on the membrane of a
93 susceptible strain *Lactococcus lactis* (21). The primary basis for the inhibitory activity of the
94 epidermin group of lantibiotics is attributed to lipid II binding and inhibition of cell wall
95 synthesis.

96 Extensive mutagenesis work has been done to generate structural variants of nisin
97 with improved bioactivities and stabilities (22, 23). Chemical modifications have also been
98 done to improve the stability of nisin by substituting the C-terminus with various lipids to
99 avoid trypsin digestion, while maintaining its inhibitory activity (24). A mutagenesis study on
100 Pep5, a member in nisin family, showed that the elimination of dehydrated residues would

101 decrease antimicrobial activity (25). Only a few single point mutations have been generated
102 on epidermin, all of which were shown to have similar or decreased inhibitory activity (26).
103 Mutagenesis studies on mutacin 1140 have revealed the importance of the lanthionine rings
104 for bioactivity. Furthermore, amino acid positions Phe1, Trp4, Dha5, and Arg13 were
105 individually modifiable, while a combination variant of Trp4 and Arg13 was inactive (27).
106 Five mutants had enhanced overall antimicrobial activity against *Micrococcus luteus*, while
107 two purified analogs had increased activities against select pathogenic bacteria. However, it
108 remained unclear if the dehydrated and protease susceptible residues at Lys2, Dha5, Arg13,
109 and Dhb14 positions are individually or collectively modifiable, and whether analogs at these
110 positions would have improvements in stability or inhibitory activity.

111 Type AI lantibiotics generally have nanomolar or submicromolar activities against
112 Gram-positive bacteria. Nisin has been used as a food preservative for over 50 years without
113 developing significant resistance (28). However, it has poor pharmacokinetics and is
114 susceptible to proteolytic degradation and oxidation. Nisin can be inactivated by
115 chymotrypsin, trypsin and thermolysin (29). Through intravenous injection in a mouse model,
116 the half-life of nisin was determined to be 0.9 h and nisin was not detectable after 3 h (30).
117 Similar with nisin, the half-life of mutacin 1140 was determined to be around 1.6 h in a rat
118 model (31). The reason for the short half-life of nisin and mutacin 1140 has not yet been
119 elucidated, the Lys and Arg residues may account for enzymatic degradation *in vivo*, while
120 dehydrated residues may be susceptible to nucleophiles present in physiological settings.
121 Furthermore, stability during drug formulation may be an issue due to intermolecular
122 reactions with nucleophiles that may result in cross-linking, generating multimolecular

123 aggregates of the antibiotic (32). Generating analogs that decrease the number of susceptible
124 residues may improve the half-life of mutacin in pharmacokinetic studies or promote the
125 stability of mutacin formulations.

126 In this study, we evaluated the importance of the residues in mutacin 1140 that
127 potentially could reduce the compounds stability. Until this study, it was not clear if the
128 dehydrated and protease susceptible residues were essential for the production and inhibitory
129 activity. Evaluating the production and activity of the analogs provided new insight into the
130 post-translational modification (PTM) machinery of mutacin 1140. Furthermore, the isolation
131 of the new mutacin 1140 analogs, provide a better understanding of the structural elements
132 within the epidermin group of lantibiotics that are important for their inhibitory activity.

133

134 **RESULTS**

135 Core peptide positions containing charged residues or dehydrated residues were
136 evaluated for their permissiveness to mutagenesis, as outlined in Figure 2.

137 **Effects of core peptide mutations on product yield.**

138 The product yield of each mutant was determined by comparing the area of the HPLC
139 fraction of the mutant analog to the area of the wild-type product, as shown in Figure 3 and
140 Suppl. Figure 1. A ratio greater than 1.0 signifies a higher yield of the mutant analog to the
141 wild-type product. Most of mutants are able to make quantifiable amount of analogs, with
142 the exception of the following mutants: S5A:T14S, S5A:T14A, S5T:T14G, S5T:T14A,

143 S5E:T14A, W4S:S5A:T14A, S5A:L6S:T14A, S5A:A12S:T14A, S5A:R13S:T13A,
144 T14A:G15A and R13A:T14A:G15A.

145 Mutations at Ser5, Thr14, or a combination of, had a variable effect on production yield
146 (Figure 3). Substitutions at the Ser5 residue were shown to improve or reduce the yield of
147 production. A S5G mutation resulted in a 67% increase in the production, while a S5E
148 mutation increased product yield by 44%. Conversely, the S5T mutation significantly
149 reduced the production by 26%. The S5G:T14G and S5G:T14A mutants resulted in a
150 statistically significant increase in yield, while the mutants S5A:R13S, S5A:T14G and
151 S5G:R13A:T14A had no statistical significant change in production compared to wild-type.
152 Several double mutant strains with amino acid substitutions at the Dha5 and Dhb14 positions
153 had lost core peptide production ability. Interestingly, four out of nine mutant strains that lost
154 core peptide production could be induced with native mutacin 1140, albeit only at levels that
155 facilitated mass spectrometry characterization. The data suggests that mutacin 1140
156 biosynthesis relies on autoinduction and that the corresponding mutant core peptides lost the
157 autoinduction activity.

158 Amino acid substitutions at the Lys2 or Arg13 residues resulted in higher product yields
159 (Figure 3). The K2A or R13A mutants had a 66% and 133% increase in the product yield,
160 respectively, while the double mutant K2A:R13A mutant had the highest increase in product
161 yield of 257%. Similarly, the mutants R13A:T14A and A12G:R13G:T14G had higher
162 production levels.

163 **Effect of core peptide mutations on PTM modifications**

164 Mass spectrometry examination of the core peptide analogs demonstrated that amino acid
165 substitutions interfered with PTM efficiency (Table 1, Suppl. Figure 2 and 3). Core peptide
166 analogs that did not have all of the serine or threonine residues undergo dehydration or
167 trapped in an intermediate stage of dehydration, and analogs that did not undergo C-terminal
168 decarboxylation were detected. The lack of a dehydration increases the predicted mass by 18
169 Da. The intermediate stage of dehydration involves the formation of a glutamylated Ser or
170 Thr residue that increases the core peptide mass by 147 Da (Figure 1A), while the lack of a
171 decarboxylation increases the mass by 46 Da. Each mutant strain's predominant product
172 based on mass spectrometry peak intensity had the expected mass, except for the G15A
173 substitution. The major product of the G15A substitution lacked a single dehydration and a
174 C-terminal decarboxylation (2342 Da). The product with the expected mass of 2280 Da was
175 the secondary product. The Gly15 residue position is crucial for the efficiency of PTMs.
176 Other single point mutations that interfered with the efficiency of the PTMs include K2A,
177 S5G, S5T, R13A, and T14G. The double and triple mutants generally produced minor
178 products lacking some of the PTMs, with the exception of A12T:T14G and
179 R13A:T14A:G15A. Interestingly, a serine residue placed at the 4^{th}, 12^{th}, or 13^{th} position were
180 dehydrated by MutB, as indicated by mutants S5A:A12S, S5A:R13S, and W4S:S5A:T14A.

181 **Bioactivity of the core peptide mutant strains.**

182 The bioactivities of *mutA* core peptide mutants and wild-type strain were determined by
183 measuring the area of zone of inhibition in the overlay assay against indicator strain *M. luteus*
184 ATCC 10240 (Figure 4 and Suppl. Figure 4). Ratio of the bioactivity of mutant to wild-type

185 with a value greater than one indicates that the area of the zone of inhibition of the mutant
186 was larger than wild-type.

187 The two trypsin susceptible residues at K2 and R13 positions were modifiable. A K2A
188 mutation resulted in a 66% increase in the overall bioactivity and the R13A mutant had an
189 87% increase in its overall bioactivity, while the double mutant K2A:R13A had an 88%
190 increase in the overall bioactivity (Figure 4). The position of the Dha5 residue in ring A
191 moderately accommodated amino acid substitutions. The S5G mutant exhibited a 20%
192 increase in its overall bioactivity against *M. luteus*. However, the S5T mutant had a 60%
193 reduction in activity compared with wild-type, while the S5E mutant was completely
194 inactive. This loss in activity suggests that bulkier side chains or a negative charge at the
195 Dha5 position may impact the inhibitory activity of the bacterium or possibly lanthionine ring
196 formation.

197 Hinge region residues were individually and collectively modifiable (Figure 4). T14G,
198 T14A and G15A exhibited similar activity as wild-type strain. A12T:T14G and T14A:G15A
199 mutants had a 17% and 40% reduction in bioactivity compared to wild-type, respectively,
200 while the R13A:T14A mutant had a 120% increase in its bioactivity. Interestingly, even when
201 the hinge region at residue positions Ala12, ArgR13, and Thr14 were changed to glycines or
202 alanines (Figure 4), the mutants exhibited slightly higher or similar level of inhibitory
203 activity. This is an interesting observation, given that the product yield of the
204 R13A:T14A:G15A mutant strain was too low to be quantified. The edge of the zone of
205 inhibition of R13A:T14A:G15A was not as clearly defined as normally observe in other
206 mutant stains, and the inhibition zone would grow in if incubated for a longer period of time

(Suppl. Figure 4G). The inhibitory activity of the mutant appeared to be bacteriostatic and not bactericidal as observed with the native compound. It is likely that the mutant product is not very stable and that this contributes to its change in bioactivity. This explanation may also explain our inability to isolate the analog product from culture.

A double mutation at the Ser5 position and the Ala12 or Arg13 position were tolerable, but the bioactivity was variable (Figure 4). Combinations of mutations at residues Dha5 and Dhb14 had a significant effect on the bioactivity of the producing strains. Several combinations of amino acid substitutions, such as S5G:T14G, S5G:T14A, S5G:R13A:T14A and S5A:T14G, maintained similar or had slightly higher bioactivity than wild-type strain. The following mutant strains were completely inactive: S5A:T14S, S5A:T14A, S5T:T14G, S5T:T14A, S5E:T14A, W4S:S5A:T14A, S5A:L6S:T14A, S5A:A12S:T14A and S5A:R13S:T14A. The data suggests that at least one Gly residue substitution in the Dha5 or Dbb14 position is required to restore the bioactivity of the mutant strains. The S5G:R13A:T14A mutant also exhibited an undefined edge on the zone of inhibition in the overlay assay (Suppl. Figure 4I), similar to what was observed for the R13A:T14A:G15A mutant strain (Suppl. Figure 4G).

Inhibitory activity of isolated core peptide analogs.

The changes in overall bioactivity of each mutant could be attributed to many factors, such as changes in the production level of mutacin 1140, changes in the bioactivity of mutacin 1140 analogs, and changes in the ability of mutacin 1140 analogs to diffuse through cell envelope and agar plates. In order to directly compare the specific activity of each

analog, all the core peptide analogs that were producible in measurable amounts were tested against a panel of Gram-positive bacteria.

All the analogs had varying level of activity and specificity against the four different bacteria tested (Table 2). Specifically, ring A analogs varied significantly in their bioactivities. S5G had a 64-fold increase in activity against *S. pneumoniae*, a two-fold increase in activity against *C. accolens*, but a two-fold decrease in activity against *M. luteus*. S5A had a four-fold increase in activity against *S. pneumoniae*, while a four-fold and two-fold decrease in activity against *M. luteus* and *S. aureus*, respectively. However, the activity of S5T analog had decreased 64-fold against *M. luteus* and decreased at least four-fold against the rest of the four strains. S5E analog was completely inactive, suggesting that the Dha5 position is extremely important for both the activity and specificity of mutacin 1140. Additional 5th position analogs were generated by thiol organosulfur labeling of the T14A analog (Suppl. Figure 5 and 2D-2F). In the T14A analog, the Dha5 residue is the only chemically susceptible residue for the organosulfur addition. Three chemicals with different physical properties were introduced into the Dha5 position, including ethanethiol (nonpolar), mercaptoethanol (polar), and thiolactic acid (negatively charged). The MIC assays against *M. luteus* ATCC 10240 (Table 4) showed that the introduction of an ethanethiol or mercaptoethanol decreased the inhibitory activity by two-fold, while the introduction of the negatively charged thiolactic acid decreased the inhibitory activity 16-fold. However, it should be noted that the S5E analog, which incorporates a carboxyl group similar to that of the thiolactic acid semisynthetic analog was completely inactive. The reason for the lack of

activity needs to be further evaluated. One possibility is that the introduction of an Asp at the fifth position interferes with the formation of ring A.

Single amino acid substitutions within hinge region changed the specificity of each analog against the different bacteria tested. R13A analog had a four-fold increase in activity against *S. pneumoniae*, while having a similar activity against *C. accolens*. T14A analog had the same activity against *S. aureus* and *S. pneumoniae*, but the activity was increased two-fold against *C. accolens*. Interestingly, T14G analog had more than a 4-fold decrease in activity against *S. aureus*, but a four-fold increase in activity against *C. accolens*. The double and triple amino acid substitutions in the hinge region had at least a two-fold decrease in activity, except for A12T:T14G and R13A:T14A. These products had a two-fold higher level of inhibitory activity against *C. accolens*.

Amino acid substitutions in both the N-terminus and hinge regions showed a decrease in activity, except for the S5A:T14G analog. This analog had the same inhibitory activity against *M. luteus* and a two-fold increase in activity against *S. pneumoniae* ATCC 27336. We also noticed that the minimal lethal concentration (MLC) was either the same or at most two-fold higher than the respective MIC values, except for the S5G:R13A:T14A analog. The MLC was eight-fold higher than the determined MIC, suggesting that this analog is bacteriostatic at the MIC.

Analogs K2A, S5G, S5A, R13A, T14G, T14A, A12G:R13G:T14G, K2A:R13A and S5A:T14G are of great interest, due to the fact that they showed improved activity and greater specificity to a pathogenic bacterial strain or they have fewer dehydrated or charged

residues in the core peptide. These mutant analogs were chosen to further evaluate their inhibitory activity against five additional *S. pneumoniae* clinical isolates (Table 3). The inhibitory activity for all the chosen analogs were worse against a majority of the *S. pneumoniae* strains except for the R13A analog. The R13A analog was either two-fold better or had the same inhibitory activity in four out of five strains tested. The K2A analog did show a two-fold improvement against the AI7 strain but showed an eight-fold or more loss in activity against the other strains tested. Interestingly, the data does demonstrate that subtle changes in the amino acid composition of the core peptide can have a significant effect on its inhibitory activity. Unfortunately, it appears that identifying an analog with improved activity against a selected species is more complicated than predicted.

Lipid II binding activity of core peptide analogs.

Several analogs, including S5E, S5G:R13A:T14A, K2A:R13A, A12G:R13G:T14G and W4A:A12T:R13D, have significantly reduced inhibitory activity compared to wild-type product. A thin-layer chromatography (TLC) assay was performed to determine if their reduction in inhibitory activity is attributed to a decrease in their ability to bind to lipid II (Suppl. Figure 6). At a molar ratio of 3:1, only wild-type mutacin 1140 retained lipid II at origin, suggesting a decrease in binding affinity of tested analogs to lipid II. The fact that K2A:R13A and A12G:R13G:T14G analogs have a reduced affinity to lipid II, suggests that positions outside the lipid II binding region (rings A & B) may also play an important role for binding to lipid II.

Evaluation of trypsin sensitivity and the development of spontaneous resistance to core peptide analogs.

Several analogs that substituted amino acids in or near the Lys2 and Arg13 residues were evaluated for trypsin sensitivity. As expected, trypsin digestion of wild-type mutacin 1140, T14A and S5A:T14G analogs did not show any resistance to trypsin cleavage, as observed in the loss of inhibitory activity (Figure 5). The K2A analog was completely inactivated with trypsin, while the R13A analog retained about 46% of its inhibitory activity. Under these experimental conditions, this observation suggests that ring A provides some protection to the nearby Lys2, and that the Arg13 residue in the hinge region is easily accessible for trypsin cleavage. As expected, the K2A:R13A analog retained approximately 89% of its inhibitory activity following trypsin treatment. Lastly, a resistance develop assay was developed to test if the positively charged residues play a role in triggering resistance development in susceptible bacteria strains. *S. aureus* ATCC 25923 was subcultured daily in subinhibitory concentrations of wild-type mutacin 1140 and R13A analog for 21 days. A two-fold increase in the MIC for wild-type was observed after four days, and this increase in resistance was maintained for the duration of the 21-day study. In the meantime, there was no observed increase in the MIC for the R13A analog during the 21-day study.

DISCUSSION

In this study, we generated single point mutations and a combination of amino acid substitutions at the N-terminus and hinge region of the lantibiotic mutacin 1140. Our findings

311 revealed that positions Lys2, Dha5, Arg13, Dhb14, and Gly15 are individually modifiable,
312 while a combination of substitutions at the Dha5 and Dhb14 positions resulted in the loss of
313 autoinducing activity or the ability to produce the lantibiotic. A single point mutation can
314 lead to the transportation of products that lack one or more PTMs. An alanine substitution at
315 the Lys2 or Arg13 position resulted in more than a two-fold increase in product isolation. In
316 some instances, a combination of amino acid substitutions yielded a core peptide with fewer
317 dehydrated or proteolytically susceptible residues with similar or enhanced inhibitory
318 activity. These analogs are of interest for future studies aimed at developing the antibiotic
319 into novel therapeutics against Gram-positive infections.

320 Nisin has been demonstrated to autoregulate its own biosynthesis by binding to the
321 transmembrane kinase NisK. The kinase phosphorylates its intracellular response regulator
322 NisR and is followed by activation of the *nis* promoter (10). Mutations in ring A (33) and C-
323 terminus (34) of nisin resulted in significantly lower or loss of auto-induction activity,
324 suggesting that autoinduction is dependent on several structural regions within nisin. Subtilin,
325 which is closely related to nisin (Figure 1B), is also an autoinducer for its own biosynthesis.
326 The F20 residue in subtilin is crucial for SpaK activation (35). The autoregulation of mutacin
327 1140 biosynthesis has not yet been clearly elucidated, but it was not surprising that mutacin
328 1140 autoregulates its production and that its autoinducing capacity is dependent on certain
329 structural regions, likely including a combination of the Dha5 and Dhb14 positions.
330 Supplementation of 100 ng/mL of wild-type mutacin 1140 promoted enough production for
331 mass characterization. The induced mutants yielded a product with the expected mass,
332 suggesting that there are no deficiencies in the PTMs. Nonetheless, the demonstration that

some mutants with substitutions in both Dha5 and Dhb14 positions lost autoinducing activity provides the basis for future studies aimed at understanding the regulation of mutacin 1140 biosynthesis. Alanine scanning mutagenesis is commonly used to determine the essential residues in lantibiotics (36, 37). However, our study shows that Gly residues are more tolerated when multiple mutations are being introduced, as was observed in the amino acid substitutions at the Dha5 and Dhb14 positions. The results suggest that glycine substitutions other than alanine substitutions should also be considered in future mutagenesis studies.

A previous study on the transportation of mutacin 1140 had mainly focused on the lanthionine-forming residues in the core peptide. Disruption of ring D resulted in the complete loss of product isolation (38). Rings A, B, and C mutants were able to produce mutacin 1140 analogs, but some lacked dehydrations and/or decarboxylation (27, 38). Our current study shows that other core peptide structural elements aside from the lanthionine rings are also essential for coordinating efficient PTMs of mutacin 1140. The biosynthetic machinery of nisin has been extensively studied (39, 40), showing that NisB and NisC are alternating enzymes, with a propensity for N-terminus to C-terminus directionality, and the dehydration and cyclization processes are not separated in time and space. However, decarboxylase does not exist in nisin biosynthetic machinery, thus little is known about the possible interaction between MutB and MutD. The PTM machinery of nisin has been shown to be relatively flexible on its substrate (41, 42). However, our study demonstrates that the PTM machinery of mutacin 1140 is not as flexible on the core peptide sequence of its substrate. Previous research on the leader peptide of mutacin 1140 (38, 43) demonstrated that the leader peptide of mutacin 1140 is twice the length of the nisin leader peptide and mutacin

1140 leader peptide contains a secondary cleavage site. Taken together, the PTM enzymes of mutacin 1140 may coordination the post-translational modifications differently from nisin.

To date, the F1I, W4A, R13D, and C-terminally modified analogs of mutacin 1140 have been purified and characterized for their bioactivity (27). In this study, more residues are evaluated for their importance on the bioactivity of the antibiotic. The 5th residue seems to be a crucial core peptide position for activity, as demonstrated by analogs S5G, S5T and S5E. The loss of activity of S5E has been attributed to the lack of lipid II binding by a TLC assay, which is in accordance with the fact that rings A and B is the lipid II binding domain of this class of lantibiotics. Interestingly, S5E analog of nisin had a two-fold increase in activity against *Streptococcus mitis* and *Bacillus cereus* (44) while the S5T mutant in nisin showed a 10-fold decrease in activity against *S. thermophiles* (45). NMR study revealed that the substitution of Dha5 to Dhb in nisin resulted in only a small chemical shift of the Leu6 residue, suggesting a negligible effect to the overall structure of the molecule (45). Given that the ring A structure of mutacin 1140 and nisin are highly similar and only differ in the fourth position (Figure 1B), much more work needs to be done to further the understanding of the importance of the Dha5 residue for lipid II binding and for the overall bioactivity of mutacin 1140.

Changes in the overall charge of mutacin 1140 plays an important role in its bioactivity. The ionic interactions of the positively charged residues Lys2 and Arg13 to the negatively charged lipids are presumably important for activity. This may explain the fact that the K2A:R13A has lower affinity to lipid II and has at least a four-fold decrease in inhibitory activity against all strains tested. Based on the predicted three-dimensional structure of

mutacin 1140 (46), the charged amino terminal of the Lys2 and Arg13 side chain are within a common plane, and this charge distribution was predicted to be important for promoting the appropriate orientation of mutacin 1140 in the lipid bilayer. Interestingly, the K2A and R13A analogs were more active against certain strains than wild-type mutacin 1140, indicating that one positive charge was sufficient to promote the membrane interaction and binding of mutacin 1140 to lipid II. A possible advantage of these analogs with fewer charged residues is the lower chance of the bacterium to develop an adaptive resistance. Teichoic acids are modulated to contain more positive charges, which is believed to prevent nisin from reaching the lipid II target (47). Sequential subculturing of *S. aureus* ATCC 25923 in subinhibitory concentrations of wild-type mutacin 1140 for 21 days led to a two-fold increase in the MIC, while there was no increase in the MIC for the R13A analog. The identified analogs with enhanced trypsin stability may also have enhanced stability in human physiological settings and less potential to trigger resistance development. These observations will need to be investigated in future experiments.

Previous mutagenesis studies of lantibiotics were to generate single point mutations in structural regions of interest or multiple amino acid substitutions within a single lanthionine ring or structural element. Very few groups have tried to construct analogs aimed at understanding the interplay of two structural regions for bioactivity. A study on a type AII lantibiotic nukacin ISK-1 constructed variants Asp13Glu:Val22Ile and His15Ser:Val22Ile that had no detectable level of product formation (48). A double mutant L6V:S16T of gallidermin produced only 8% of the level of wild-type product, thus its bioactivity was not determined (26). A mutacin 1140 analog W4A:R13D did not have any inhibitory effect

against *M. luteus* (27). A double mutation within rings AB and CD of mutacin 1140 resulted in completely lost of bioactivity (38). In this study, we successfully generated bioactive analogs of mutacin 1140 with substitutions in the lipid II binding and hinge region. The study provided a better understanding for the limitations in mutacin 1140 mutagenesis and the importance for two distinct structural regions for the inhibitory and autoinduction activity. Our *in vitro* protease stability study, suggests that the removal of the Lys2 and Arg13 residues improves the core peptide's stability. The generation of mutacin 1140 analogs with fewer chemically active vinyl groups as well as fewer protease susceptible residues will provide a basis for the future study aimed at evaluating the hypothesis that these susceptible residues may play a role in the short half-life of mutacin 1140 *in vivo*.

MATERIALS AND METHODS

Bacterial strains and growth conditions

Bacterial strains and plasmids used are listed in Table 5. The pCR™4-TOPO® TA vector, pCR™2.1-TOPO® TA vector (Invitrogen, Carlsbad, CA), and pMiniT™ vector (NEB, Ipswich, MA) were used as described by the manufacturer. *Escherichia coli* DH5α, TOP10 (Invitrogen, Carlsbad, CA) and 10β (NEB, Ipswich, MA) were used as host for the vectors and were cultured in LB agar or broth. *Streptococcus mutans* JH1140, *Micrococcus luteus* ATCC 10240, *Staphylococcus aureus* ATCC 25923, *Streptococcus pneumoniae* ATCC 27336, *Streptococcus pneumoniae* AI6 and AI7 were cultured on Todd-Hewitt yeast extract (THyex) agar plates (containing 30 g/L Todd-Hewitt broth and 3 g/L yeast extract and 15 g/L

420 agar) or in THyex broth (containing 30 g/L Todd-Hewitt broth, 3 g/L yeast extract).
421 *Corynebacterium accolens* KPL1818 (49) is fatty acid synthase-deficient, and the THyex
422 broth or agar was supplemented with 1% of Tween 80 to promote the bacteria growth. *S.*
423 *pneumoniae* AI8, AI11, and AI14 were cultured in THyex broth supplemented with 5%
424 human blood, or on Blood Agar plates. All bacterial strains were cultured at 37°C.

425 **Site-directed mutagenesis of *mutA***

426 The *S. mutans mutA* gene cluster (50) was used to design primers (listed in Table 6) for the
427 mutagenesis and sequencing. The *mutA* is the structural gene encoding the prepeptide of
428 lantibiotic mutacin 1140 in *S. mutans* JH1140. Site-directed mutations were introduced into
429 the core peptide region of *mutA* by overlap PCR. PCR product containing desired mutations
430 and its upstream and downstream fragments (~500 bp) were inserted into pCR^{TM}4-TOPO®,
431 pCR^{TM}2.1-TOPO® or pMiniT vector, and transformed into competent *E. coli* cells following
432 the manufacturers' instructions. The *S. mutans* strain *ΔmutA*/IFDC2 was used for
433 transformation as previously described with minor modifications (38). Briefly, pIFDC2 is a
434 hybrid positive- and negative-selection cassette (51) using a highly expressed *S. mutans*
435 lactate dehydrogenase (ldh) promoter to drive the expression of a positive selection marker
436 (*ermAM*) and a negative selection marker (-*pheS**). Fragments of ~500 bp of the upstream
437 and downstream of *mutA* were attached to IFDC2 cassette respectively by overlap PCR,
438 introduced into *S. mutans*, and resulted in *S. mutans ΔmutA*/IFDC2. Plasmids containing the
439 desired mutations were introduced into *S. mutans* Δ*mutA*/IFDC2, and the recombination in *S.*
440 *mutans* enabled screening for the desired mutations within *mutA*. To activate the natural
441 competence pathway and transform plasmids into *S. mutans*, a synthetic competent-

stimulating peptide (CSP), obtained from Peptides & Elephants (German)) was added as previously described (52). An overnight culture of *S. mutans* Δ*mutA*/IFDC2 in THyex broth was diluted to OD_{600} 0.1 and grown to OD_{600} 0.2, after which 5 µl of 10 µg/ml CSP was added to 200 µl of the bacterial culture. After 30 min of incubation at 37°C, 5 µl of extracted plasmid was added to the cell culture. Following 3 h of incubation, the culture was diluted 10-fold and 50 µl of the sample was plated onto a THyex agar plate containing 4 mg/ml of p-chlorophenylalanine. Colonies grew up after 2 days indicate the loss of *-pheS** and the occurrence of recombination. To remove false positives, replicate plates of colonies on both THyex and THyex with 15 µg/ml erythromycin plates were incubated for 2 days. Positive transformants that did not grow on erythromycin plates were streaked again onto fresh THyex agar plate and the mutation was confirmed by PCR and sequencing.

Determination of the bioactivity of the mutant core-peptide strains

The deferred antagonism assay was used to determine the bioactivity of mutants as previously described (27). Briefly, *S. mutans* wild-type and mutants were grown overnight in THyex broth gently shaking at 37°C. The culture was then diluted to OD_{600} 0.1 and grown to OD_{600} 0.6-0.8. After diluting again to OD_{600} 0.2, 2 µl of each culture was spotted on a pre-warmed THyex agar plate and allowed to air dry. The plate was inverted and incubated at 37°C for 18 h in an anaerobic jar before being heat killed at 65°C for 30 min. The indicator strain *M. luteus* ATCC 10240 was grown to OD_{600} 0.6 and diluted to OD_{600} 0.2. Subsequently, 400 µl of the bacteria culture was added to every 10 ml of molten THyex top agar (0.75% agar). 5 ml of the indicator strain in top agar was poured over the surface of each THyex agar plate. After solidifying, the plate was inverted and incubated for 18 hrs at 37°C.

464 The area of zone of inhibition for each mutant was measured and compared to that of the
465 zone of inhibition for the wild-type JH1140 strain. Experiments were done in triplicate.
466 Student *t*-test was used to determine statistical significance ($P < 0.05$).

467 **Purification of mutacin 1140 and its analogs**

468 Purification of mutacin 1140 analogs was performed as previously described (27). Briefly, *S.*
469 *mutans* strains were grown on a modified THyex soft agar containing 30 g/L Todd Hewitt,
470 3 g/L yeast extract, 1 g/L KH_2PO_4, 0.1 g/L K_2HPO_4, 0.3 g/L $MgSO_4$, 0.005 g/L $FeSO_4$,
471 0.005 g/L $MnSO_4$, and 0.3% agar. In cases when no product was detected for a mutant strain,
472 the soft agar was supplemented with wild-type mutacin 1140 (100 ng/ml) as an inducer for
473 production. The media was stab inoculated with *S. mutans* strain and was incubated at 37°C
474 for 3 days. After that, the media was immediately frozen at -80°C overnight and was thawed
475 the next day in a 65°C incubator. The thawed media was centrifuged at 20,000 g for 30 min
476 at 4°C in 250 ml centrifuge bottles to remove agar and cell pellets (Beckman J2-21
477 Centrifuge). The supernatant was mixed with an equal volume of chloroform and shaken
478 vigorously for several times. The mixture was again centrifuged at 20,000 g for 30 min at
479 4°C. The clear aqueous phase and chloroform phase was poured out immediately after
480 centrifugation and the white precipitant phase between the aqueous and chloroform layers
481 was collected and allowed to air dry. The dried material was resuspended in 5 ml of 35%
482 acetonitrile/water (vol/vol) with 0.1% trifluoroacetic acid (TFA). The remaining insoluble
483 material was removed by centrifugation at 15,000 g for 10 min (Eppendorf Centrifuge 5424).
484 The sample was run on either a semi-prep C18 column (Agilent® ZORBAX, (Agilent
485 Technologies, Santa Clara, CA) ODS, C18, 5 µm, 4.6 × 250 mm) or analytical column as

previously reported (27). All solvents for HPLC contain 0.1% TFA. The sample was separated through a water/ACN gradient starting from 95% to 75% water over 10 min, an isocratic flow at 75% water for 5 min, followed by a linear gradient from 75% to 5% water over 35 min. The fractions eluted between 60-45% water and were analyzed by mass-spectrometry. The desired fractions were dried by lyophilization and resuspended in 1 ml of 35% ACN with 0.1% TFA. The samples were rerun on an analytical column with the same gradient, or a modified linear water/ACN gradient starting from 90% to 20% water over 30 min. The productivity of each analog was quantified by comparing the peak area of each analog to the peak area of wild-type mutacin 1140. Extractions were done in triplicate. Student *t*-test was used to determine statistical significance ($P < 0.05$).

Mass Spectrometry

Shimadzu/Kratos MALDI-TOF mass spectrometer or ThermoFisher DecaXP ion trap mass spectrometer was used to determine the mass of each RP-HPLC core peptide fraction. Briefly, for the MALDI-TOF mass spectrometer, 1 µl of each fraction was directly mixed with 1 µl of α-cyano-4-hydroxycinnamic acid matrix (30 mg/ml in MeOH-0.1% TFA and then dilute with 50% ACN/water with 0.1% TFA to a 6 mg/ml concentration) and dried on the MALDI-TOF target plate in a 37°C incubator. MALDI-TOF MS was operated in the positive linear mode or reflective mode. For the ThermoFisher DecaXP ion trap mass spectrometer, around 1 µg of dried purified material was resuspended in 100 µl of 50% ACN/water (vol/vol) and the masses were determined by direct infusion. Instrument was used in positive mode was used and the chromatograph was recorded at a 0.5 min time frame. Wild-type mutacin 1140 was used as a mass standard and control.

508 **Minimum inhibitory concentration and minimum lethal concentration assays**

509 The mutacin 1140 analogs were dried and weighed on an analytical balance (Ohaus). The
510 concentration of samples (＜1 mg in weight) were determined by Bradford assay using
511 mutacin 1140 wild-type as standard following the manufacturer's instruction (Quick Start™,
512 Bio-rad). The minimal inhibitory concentration (MIC) is the lowest concentration of
513 compound that inhibits the visible growth of the bacteria after 24 hours of incubation, and
514 was performed following a modified version of the broth microdilution method described in
515 M07-A8 by the Clinical Laboratory Standards Institute (53).The minimum lethal
516 concentration (MLC) was determined by plating 50 µl of culture media on THyex plates at
517 2× and 1× of the determined MIC concentration, with the exception of S5G:R13A:T14A,
518 which was plated until 8× of the determined MIC. The concentration in which no colony
519 forming units formed on the plates after 24 hours was determined to be the MLC. The MICs
520 of mutacin 1140 wild-type and analogs were first determined against *M. luteus* ATCC 10240,
521 *S. aureus* ATCC 25923, *S. pneumoniae* ATCC 27336, and *C. accolens* KPL 1818. The
522 mutacin 1140 analogs of particular interest were selected and tested against five additional *S.*
523 *pneumoniae* strains, including AI6, AI7, AI8, AI11 and AI14. All experiments were done at
524 least in duplicate.

525 **Thiol organosulfur labeling of mutacin 1140 analog T14A**

526 Thiol organosulfur additions occur readily at room temperature to the vinyl groups within
527 Dha and Dhb residues. Tris buffer (pH 8.5) was used to keep the thioether linkages intact
528 during the thiol addition reaction. The Dha5 residue in the T14A analog was chemically

529 modified with thiol compounds containing different physical properties: non-polar, polar, and
530 charged. These compounds were ethanethiol, β-mercaptoethanol, and thiolactic acid, as
531 previously described (46) with some minor modifications. Briefly, T14A analog was
532 incubated in 200 mM Tris buffer pH 8.5 with 10-fold excess of thiol compound (molar ratio)
533 in a glass vial perfused with Helium at room temperature for 2 hours. Samples were then
534 purified by ZipTip (Pierce™ C18 Tips, #87782, ThermoFisher Scientific) and analyzed by
535 MALDI-TOF MS. The concentration of each sample was quantified by Bradford assay using
536 wild-type mutacin 1140 as a standard following the manufacturer's instruction (Quick
537 Start™, Bio-rad).

538 **Trypsin stability of selected mutacin 1140 analogs**

539 The trypsin stability of mutacin 1140 analogs was tested as previously described with minor
540 modifications (54). Briefly, a 2x stock solution of sodium phosphate buffer (0.134 M, pH 7.6)
541 and a 10x trypsin stock solution (5.19 mg of trypsin in 1 mL 1 mM HCl solution) were used.
542 A 100 µl reaction mixture was made in 1.8 mL centrifuge tubes (VWR, Cat#89000-028),
543 consisting of 10 µl of the 10x protease stock solution, 50 µl 2x stock solution, 39 µL ddH2O,
544 and 1 µL DMSO. Reaction mixture without protease was made in the same way, except that
545 10 µl of 1 mM HCl was used instead of the 10x trypsin stock solution. 1 µg of each analog
546 was added to reaction mixtures with and without trypsin, and all tubes were incubated for 30
547 min at 37°C. An antagonism assay was used to determine the bioactivity of trypsin digested
548 mutacin 1140 analogs as previously described with minor modifications (27). Briefly, a
549 single colony of the indicator strain *M. luteus* ATCC 10240 was inoculated onto 5 ml of
550 THyex broth, grown to OD_{600} of 0.6 and diluted to OD_{600} of 0.2. Subsequently, 400 µl of

bacteria culture was added to every 10 ml of molten THyex top agar (0.75% agar), and poured over the surface of the plate as described above. After solidifying, 10 µl of the reaction mixtures, with and without protease, were spotted onto the bioassay plate. Once the spots were dry, the plates were inverted and incubated overnight at 37°C. The area of zone of inhibition after treatment relative to the zone of inhibition of the material before treatment was used as an indication of protease stability. A value of 1.0 (or 100%) would indicate that the analog retained all of its bioactivity following trypsin exposure, while a value of 0 (or 0%) would indicate the analog was completely inactivated by trypsin. A duplicate set of experiments were performed.

Lipid II binding assay

A lipid II binding assay using a thin-layer chromatography (TLC) procedure has been performed as previously described (55) with minor modifications. Briefly, the mobile solvent used consists of butanol-acetic acid-water-pyridine in a 15:3:12:10 volume ratio. The reaction mixture was made in 10 µl of mobile solvent consisting of 0.2 mM lipid II and 0.6 mM peptide in glass vials. Peptides include wild-type mutacin 1140, S5E, S5G:R13A:T14A, K2A:R13A, A12G:R13G:T14G, and W4A:A12T:R13D. Experimental controls included lipid II and each peptide spotted separately. The reaction mixture was incubated for 2 hours at room temperature before spotting approximately 10 µl on the TLC plate. The spotted samples were allowed to air dry before the plate was inserted into a chamber containing the mobile solvent. The mobile solvent was allowed to run until it reach approximately 2 cm from the top of the plate. The plate was removed and air dried before being stained in an iodine chamber for visualization.

ACKNOWLEDGEMENTS

We thank Katherine Lemon, Department of Microbiology at the Forsyth Institute, for the use of her Corynebacterium strain and we also would like to thank Bindu Nanduri, Department of Basic Sciences at Mississippi State University for use of her clinical *S. pneumoniae* strains. We thank Eefjan Breukink, Department of Chemistry at Utrecht University, for the lipid II. We have no conflicts of interest to declare. Experiments were supported by NIH grants 1R41AI131792-01 and 1R41AI122441-01A1.

582 **Table 1** Mass of mutacin 1140 analogs. * represents the requirement of wild-type mutacin
583 1140 as an inducer; "a" represents the lack of C-terminal decarboxylation; "b" represents the
584 lack of one or more dehydration; "c" represents the presence of glutamylated S/T residues.
585 Predicted mass is based on the mass observed for wild-type mutacin 1140, which serves as a
586 standard.

Mu1140 analogs	Predicted (Da)	Measured (Da)
Wild-type	2266	2266
Single point mutation		
K2A	2209	2209; 2255a
S5G	2254	2254; 2300a; 2551c
S5E	2326	2326
S5T	2275	2275; 2292b; 2440b,c; 2483a,b,c
R13A	2181	2181;2513b,c
T14G	2241	2240; 2302a,b
T14A	2252	2252
G15A	2280	2342a,b; 2280
Mutations in hinge region		
A12T:T14G	2252	2252
R13A:T14A	2169	2169; 2186b
T14A:G15A	2263	2262; 2452a,c; 2473a,b,c
A12G:R13G:T14G	2127	2127; 2181b; 2503a,b,c
R13A:T14A:G15A	2183	2183
Mutations in both N-terminus and hinge region		
K2A:R13A	2124	2124; 2142b; 2187a,b
S5A:A12S	2261	2262; 2280b
S5A:R13S	2178	2178; 2196b; 2326c
S5G:T14G	2228	2228
S5G:T14A	2237	2238; 2429a,c
S5G:R13A:T14A	2157	2157
S5A:T14G	2242	2242
S5A:T14S*	2252	2253
S5A:T14A*	2253	2253
S5T:T14G	2254	No Product
S5T:T14A	2268	No Product
S5E:T14A	2314	No Product
W4S:S5A:T14A*	2139	2137
W4A:A12T:R13D	2119	2119
S5A:L6S:T14A	2209	No Product
S5A:A12S:T14A	2252	No Product
S5A:R13S:T14A*	2168	2169

587

588

589 **Table 2** MIC and MLC (μg/ml) of mutacin 1140 analogs against four indicator strains.

	M. luteus ATCC 10240		*S. aureus* ATCC 25923		*C. accolens* KPL 1818		*S. pneumoniae* ATCC 27336	
Mu1140 analogs	MIC	MLC	MIC	MLC	MIC	MLC	MIC	MLC
WT	0.0625	0.0625	8	8	1	2	0.5	0.5
K2A	0.25	0.5	32	32	4	4	0.25	0.25
S5G	0.125	0.125	8	8	0.5	0.5	0.0078	0.0078
S5A	0.25	0.5	16	16	1	1	0.125	0.125
S5T	4	4	>32	>32	>4	>4	2	2
R13A	0.0625	0.0625	16	16	1	1	0.125	0.125
T14G	0.0625	0.0625	>32	>32	0.25	0.5	0.5	0.5
T14A	0.125	0.125	8	16	0.5	2	0.5	0.5
G15A	0.125	0.125	16	16	1	2	0.5	0.5
A12T:T14G	0.25	0.25	>32	>32	0.5	1	2	2
R13A:T14A	0.25	0.5	32	32	0.5	0.5	2	2
A12G:R13G:T14G	0.5	1	32	32	2	2	1	1
K2A:R13A	0.25	0.25	>32	>32	>4	>4	2	2
S5A:A12S dehydrated	0.125	0.25	16	32	0.5	1	0.125	0.125
S5A:A12S	0.125	0.25	16	16	0.5	1	0.125	0.125
S5A:R13S	0.125	0.25	>32	>32	2	4	0.5	0.5
S5G:T14G	0.5	0.5	8	16	0.5	1	2	2
S5G:T14A	0.125	0.125	>32	>32	>4	>4	4	4
S5G:R13A:T14A	2	16	>32	>32	>4	>4	8	>16
S5A:T14G	0.0625	0.125	32	32	0.5	1	0.25	0.25

590

591

592

593 **Table 3** MICs (μg/ml) of selected mutacin 1140 analogs against five
594 additional *S. pneumoniae* strains.

Mu1140 analogs	AI6	AI7	AI8*	AI11*	AI14*
WT	1	0.25	1	1	0.125
K2A	8	0.125	8	8	>8
S5G	>8	2	>8	8	>8
S5A	8	2	8	8	>8
R13A	0.5	0.25	0.5	0.5	0.25
T14G	8	8	8	1	1
T14A	8	8	8	4	2
A12G:R13G:T14G	8	8	>8	4	>8
K2A:R13A	4	4	32	16	64
S5A:T14G	>8	8	>8	>8	>8

595 * MIC for the *S. pneumoniae* strains were tested in the presence of 5% human
596 blood to promote growth.

597

598 **Table 4** Mass of mutacin 1140 analogs generated by thiol organosulfur labeling and their
599 bioactivity against selected bacteria.

Mu1140 analogs	Expected mass (Da)	Observed mass (Da)	*M. luteus* ATCC 10240 MIC (µg/ml)
Wild-type	2266	2264	0.0625
T14A	2254	2252	0.125
T14A - ethanethiol	2316	2315	0.25
T14A - mercaptoethanol	2332	2329	0.25
T14A - thiolactic acid	2360	2359	2

600
601

602 **Table 5** Strains used in this study.

Strain	Characteristic	Reference and/or source[a]
E. coli DH5α	Cloning host (pCR2.1-TOPO, pCR4-TOPO)	Invitrogen
E. coli 10β	Cloning host (pMiniT)	NEB
M. luteus ATCC 10240	Indicator strain for overlay assay	ATCC
C. accolens KPL 1818		49&FI
S. aureus ATCC 25923		ATCC
S. pneumoniae ATCC 27336		ATCC
S. pneumoniae AI6		MSU
S. pneumoniae AI7		MSU
S. pneumoniae AI8		MSU
S. pneumoniae AI11		MSU
S. pneumoniae AI14		MSU
S. mutans JH1140 (ATCC	Wild-type strain that produces mutacin 1140	ATCC
JH1140 *mutA*/IFDC2	Gene replacement strain	38
JH1140 S5A	mutA::S5A site-directed derivative	27
JH1140 W4A:A12T:R13D	mutA::W4A:A12T:R13D site-directed derivative	27
JH1140 K2A	mutA::K2A site-directed derivative	This study
JH1140 S5G	mutA::S5G site-directed derivative	This study
JH1140 S5T	mutA::S5T site-directed derivative	This study
JH1140 S5E	mutA::S5E site-directed derivative	This study
JH1140 R13A	mutA::R13A site-directed derivative	This study
JH1140 T14G	mutA::T14G site-directed derivative	This study
JH1140 T14A	mutA::T14A site-directed derivative	This study
JH1140 G15A	mutA::G15A site-directed derivative	This study
JH1140 A12T:T14G	mutA::A12T:T14G site-directed derivative	This study
JH1140 R13A:T14A	mutA::R13A:T14A site-directed derivative	This study
JH1140 T14A:G15A	mutA::T14A:G15A site-directed derivative	This study
JH1140 A12G:R13G:T14G	mutA::A12G:R13G:T14G site-directed derivative	This study
JH1140 R13A:T14A:G15A	mutA::R13A:T14A:G15A site-directed derivative	This study
JH1140 K2A:R13A	mutA::K2A:R13A site-directed derivative	This study
JH1140 S5A:A12S	mutA::S5A:A12S site-directed derivative	This study
JH1140 S5A:R13S	mutA::S5A:R13S site-directed derivative	This study
JH1140 S5G:T14G	mutA::S5G:T14G site-directed derivative	This study
JH1140 S5G:T14A	mutA::S5G:T14A site-directed derivative	This study
JH1140 S5G:R13A:T14A	mutA::S5G:R13A:T14A site-directed derivative	This study
JH1140 S5A:T14G	mutA::S5A:T14G site-directed derivative	This study
JH1140 S5A:T14S	mutA::S5A:T14S site-directed derivative	This study
JH1140 S5A:T14A	mutA::S5A:T14A site-directed derivative	This study
JH1140 S5T:T14G	mutA::S5T:T14G site-directed derivative	This study
JH1140 S5T:T14A	mutA::S5T:T14A site-directed derivative	This study
JH1140 S5E:T14A	mutA::S5E:T14A site-directed derivative	This study
JH1140 W4S:S5A:T14A	mutA::W4S:S5A:T14A site-directed derivative	This study
JH1140 S5A:L6S:T14A	mutA::S5A:L6S:T14A site-directed derivative	This study
JH1140 S5A:A12S:T14A	mutA::S5A:A12S:T14A site-directed derivative	This study
JH1140 S5A:R13S:T14A	mutA::S5A:R13S:T14A site-directed derivative	This study

603 [a]: MSU, Department of Pathobiology and Population Medicine at Mississippi State University; FI,
604 Department of Microbiology at the Forsyth Institute.

605

606

Applied and Environmental Microbiology

607 **Table 6.** Primers used in this study.

Primer	Sequence (5' - 3')
MutA UpF	GTT GAA GAA ATA AAT CCT ACG ATT GCT TC
MutA DnR	GAT TTA ACT GTG ATG TCC TCA TGA ATA T
MutA UpF-2	AGT TTT AGC CAT TAA AGC CAT CTT G
MutA DnR-2	CGA TGG ACG AAA ACA AGC C
LanR	AAA AGT TGC CTA ATG GTT TTC TG
MutA Seq	AGA GGC TAA TGG TGG TAT TAT ATT ATT G
K2A-F	ACG ATC CAG ATA CTC GTT TCG CAA GTT GGA GCC TTT GTA CG
K2A-R	CGT ACA AAG GCT CCA ACT TGC GAA ACG AGT ATC TGG ATC GT
S5G-F	CAG ATA CTC GTT TCA AAA GTT GGG GCC TTT GTA CGC CTG G
S5G-R	CCA GGC GTA CAA AGG CCC CAA CTT TTG AAA CGA GTA TCT G
S5T-F	AGA TAC TCG TTT CAA AAG TTG GAC CCT TTG TAC GCC TGG TTG
S5T-R	CAA CCA GGC GTA CAA AGG GTC CAA CTT TTG AAA CGA GTA TCT
S5E-F	CAG ATA CTC GTT TCA AAA GTT GGG AAC TTT GTA CGC CTG GTT GT
S5E-R	ACA ACC AGG CGT ACA AAG TTC CCA ACT TTT GAA ACG AGT ATC TG
A12S-F	CTT TGT ACG CCT GGT TGT TCA AGG ACA GGT AGT TTC AAT AGT TA
A12S-R	TAA CTA TTG AAA CTA CCT GTC CTT GAA CAA CCA GGC GTA CAA AG
R13S-F	CGC CTG GTT GTG CAA GCA CAG GTA GTT TCA ATA GTT ACT GTT G
R13S-R	CAA CAG TAA CTA TTG AAA CTA CCT GTG CTT GCA CAA CCA GGC G
R13A-F	GTA CGC CTG GTT GTG CAG CTA CAG GTA GTT TCA ATA G
R13A-R	CTA TTG AAA CTA CCT GTA GCT GCA CAA CCA GGC GTA C
T14G-F	GCC TGG TTG TGC AAG GGG AGG TAG TTT CAA TAG TTA CTG TTG C
T14G-R	GCA ACA GTA ACT ATT GAA ACT ACC TCC CCT TGC ACA ACC AGG C
T14S-F	GCC TGG TTG TGC AAG GAG CGG TAG TTT CAA TAG TTA CTG TTG C
T14S-R	GCA ACA GTA ACT ATT GAA ACT ACC GCT CCT TGC ACA ACC AGG C
T14A-F	ACG CCT GGT TGT GCA AGG GCA GGT AGT TTC AAT AGT TAC TG
T14A-R	CAG TAA CTA TTG AAA CTA CCT GCC CTT GCA CAA CCA GGC GT
G15A-F	GCC TGG TTG TGC AAG GAC AGC TAG TTT CAA TAG TTA CTG TTG C
G15A-R	GCA ACA GTA ACT ATT GAA ACT AGC TGT CCT TGC ACA ACC AGG C
R13A:T14A-F	ACG CCT GGT TGT GCA GCG GCA GGT AGT TTC AAT AGT TAC TGT TGC
R13A:T14A-R	GCA ACA GTA ACT ATT GAA ACT ACC TGC CGC TGC ACA ACC AGG CGT
T14A:G15A-F	GCC TGG TTG TGC AAG GGC AGC TAG TTT CAA TAG TTA CTG TTG CTG ATT G
T14A:G15A-R	CAA TCA GCA ACA GTA ACT ATT GAA ACT AGC TGC CCT TGC ACA ACC AGG C
A12G:R13G:T14G-F	CTT TGT ACG CCT GGT TGT GGA GGG GGA GGT AGT TTC AAT AGT TAC TGT TGC
A12G:R13G:T14G-R	GCA ACA GTA ACT ATT GAA ACT ACC TCC CCC TCC ACA ACC AGG CGT ACA AAG
R13A:T14A:G15A-F	CGC CTG GTT GTG CAG CGG CAG CTA GTT TCA ATA GTT ACT GTT GCT G
R13A:T14A:G15A-R	CAG CAA CAG TAA CTA TTG AAA CTA GCT GCC GCT GCA CAA CCA GGC G
W4S:S5A-F	CAA AAG TTC GGC CCT TTG TA
W4S:S5A-R	TAC AAA GGG CCG AAC TTT TG
S5A:L6S-F	AAG TTG GGC CAG TTG TAC GC
S5A:L6S-R	GCG TAC AAC TGG CCC AAC TT

A12S:T14A-F	TGG TTG TTC AAG GGC AGG TA
A12S:T14A-R	TAC CTG CCC TTG AAC AAC CA
R13S:T14A-F	GTT GTG CAA GCG CAG GTA GT
R13S:T14A-R	ACT ACC TGC GCT TGC ACA AC

608

609

610 **Figure 1.** Structural elements found in type AI lantibiotics. (A) Representation of the
611 dehydration mechanism of dehydratase LanB in type AI lanthipeptides. The mass difference
612 between the intermediate in the dehydration process and the final product is 147 Da. (B)
613 Primary sequence alignment of nisin family and epidermin family of type AI lantibiotics.
614 Lipid II binding domain is shaded grey. Lanthionine rings are shown by black lines.
615 Epidermin and gallidermin are highly similar to mutacin 1140. The residues that are different
616 between gallidermin and mutacin 1140 are underlined. (C) A representative covalent
617 structure of mutacin 1140. The four lanthionine rings are labeled as A, B, C, and D. The lipid
618 II binding domain consists of the rings A and B, while the lateral assembly domain consists
619 of the hinge region (residues 12-15) and rings C and D. Protease susceptible residues Lys and
620 Arg are shown in bold, while dehydrated residues Dha and Dhb are shown in bold and italic.
621
622 **Figure 2.** Summary of the mutacin 1140 core peptide mutants generated in this study. Single
623 core peptide amino acid substitutions and multiple amino acid substitutions in the hinge
624 region are shown above the provided mutacin 1140 sequence, while multiple substitutions in
625 both the N-terminus and hinge region are shown below the mutacin 1140 sequence. Each lane
626 represents one single core peptide mutant. Bold amino acid abbreviations represent mutant
627 strains with significantly increased bioactivity, grey represents mutant strains with
628 significantly decreased bioactivity, and underlined represents mutant strains that are inactive.
629 The rest of the mutant strains presented had no statistical significant change in bioactivity
630 against the indicator strain *M. luteus* ATCC 10240.
631
632 **Figure 3.** Production level of the mutant *mutA* core peptide compare to the production of
633 wild-type core peptide. (A) Single point mutations in core peptide; (B) Multiple amino acid
634 substitution mutations in the hinge region; (C) Multiple amino acid substitution mutations
635 within the N-terminus and hinge region. Three independent extractions were quantified by
636 measuring RP-HPLC peak area at 220 nm. The ratio of the peak areas of the mutacin 1140
637 analogs to the peak area of wild-type mutacin 1140 are shown. The student *t* test was used for
638 statistical analyses, and the asterisks signify statistical significance ($p < 0.05$).
639
640 **Figure 4.** Bioactivity of *mutA* core peptide mutant strains compared to wild-type *S. mutans*
641 JH1140. (A) Single point mutations in the core peptide; (B) Multiple amino acid substitution
642 mutations in the hinge region; (C) Multiple amino acid substitution mutations within the N-
643 terminus and hinge region. The bioactivities of the mutants were measured as the ratio of the
644 area of the zone of inhibition of each mutant strain relative to the area of the wild-type strain.
645 A value greater than 1.0 would indicate that the mutant strain is more active than the wild-
646 type strain. *M. luteus* ATCC 10240 was used as the indicator strain for antimicrobial activity
647 and experiments were done in triplicate. The student *t* test was used for statistical analysis,
648 and the asterisks signify statistical significance ($p < 0.05$).
649
650 **Figure 5.** Trypsin stability of selected mutacin 1140 analogs. Wild-type mutacin 1140, K2A,
651 R13A, K2A:R13A, T14A, and S5A:T14G were tested. The bioactivity following trypsin
652 digestion was measured as the ratio of the area of the zone of inhibition of trypsin treated
653 analog to the untreated analog. A value of 1.0 would indicate that the analog retained 100%

of activity following trypsin exposure. *M. luteus* ATCC 10240 was used as the indicator strain for antimicrobial activity. The experiments were done in duplicate.

658 **REFERENCES**

1. Schnell, N., Entian, K. D., Schneider, U., Götz, F., Zähner, H., Kellner, R., Jung, G. 1988. Prepeptide sequence of epidermin, a ribosomally synthesized antibiotic with four sulphide-rings. Nature, 333: 276.
2. Chatterjee, C., Paul, M., Xie, L., van der Donk, W. A. 2005. Biosynthesis and mode of action of lantibiotics. Chemical reviews, 105:633-684.
3. Engelke, G., Gutowski-Eckel, Z., Hammelmann, M., Entian, K. D. 1992. Biosynthesis of the lantibiotic nisin: genomic organization and membrane localization of the NisB protein. Applied and Environmental Microbiology, 58: 3730-3743.
4. Kluskens, L. D., Kuipers, A., Rink, R., de Boef, E., Fekken, S., Driessen, A. J., Moll, G. N. 2005. Post-translational modification of therapeutic peptides by NisB, the dehydratase of the lantibiotic nisin. Biochemistry, 44:12827-12834.
5. Garg, N., Salazar-Ocampo, L. M., Van Der Donk, W. A. 2013. In vitro activity of the nisin dehydratase NisB. Proceedings of the National Academy of Sciences, 110: 7258-7263.
6. Li, B., Yu, J. P. J., Brunzelle, J. S., Moll, G. N., Van Der Donk, W. A., Nair, S. K. 2006. Structure and mechanism of the lantibiotic cyclase involved in nisin biosynthesis. Science, 311, 1464-1467.
7 Klein, C., Kaletta, C., Schnell, N., Entian, K. D. 1992. Analysis of genes involved in biosynthesis of the lantibiotic subtilin. Applied and environmental microbiology, 58: 132-142.
8. Kupke, T., Stevanović, S., Sahl, H. G., Götz, F. 1992. Purification and characterization of EpiD, a flavoprotein involved in the biosynthesis of the lantibiotic epidermin. Journal of bacteriology, 174, 5354-5361.
9. Ortega, M. A., Hao, Y., Zhang, Q., Walker, M. C., Van Der Donk, W. A., Nair, S. K. 2015. Structure and mechanism of the tRNA-dependent lantibiotic dehydratase NisB. Nature, 517, 509.
10. Kuipers, O. P., Beerthuyzen, M. M., de Ruyter, P. G., Luesink, E. J., de Vos, W. M. 1995. Autoregulation of nisin biosynthesis in Lactococcus lactis by signal transduction. Journal of Biological Chemistry, 270, 27299-27304.
11. Hillman, J. D., Novák, J., Sagura, E., Gutierrez, J. A., Brooks, T. A., Crowley, P. J., Bleiweis, A. S. 1998. Genetic and biochemical analysis of mutacin 1140, a lantibiotic from Streptococcus mutans. Infection and immunity, 66: 2743-2749.
12. Kreth, J., Merritt, J., Shi, W., Qi, F. 2005. Competition and coexistence between Streptococcus mutans and Streptococcus sanguinis in the dental biofilm. Journal of bacteriology, 187: 7193-7203.
13. Merritt, J., Kreth, J., Shi, W., Qi, F. 2005. LuxS controls bacteriocin production in Streptococcus mutans through a novel regulatory component. Molecular microbiology, 57: 960-969.
14. Merritt, J., Qi, F. 2012. The mutacins of Streptococcus mutans: regulation and ecology. Molecular oral microbiology, 27: 57-69.

15 Brötz, H., Josten, M., Wiedemann, I., Schneider, U., Götz, F., Bierbaum, G., Sahl, H. G. 1998. Role of lipid - bound peptidoglycan precursors in the formation of pores by nisin, epidermin and other lantibiotics. Molecular microbiology, 30: 317-327.

16 Breukink, E., Wiedemann, I., Van Kraaij, C., Kuipers, O. P., Sahl, H. G., De Kruijff, B. 1999. Use of the cell wall precursor lipid II by a pore-forming peptide antibiotic. Science, 286: 2361-2364.

17. Hsu, S. T. D., Breukink, E., Tischenko, E., Lutters, M. A., de Kruijff, B., Kaptein, R., van Nuland, N. A. 2004. The nisin–lipid II complex reveals a pyrophosphate cage that provides a blueprint for novel antibiotics. Nature structural & molecular biology, 11:963-967.

18. Hasper, H. E., Kramer, N. E., Smith, J. L., Hillman, J. D., Zachariah, C., Kuipers, O. P., Breukink, E. 2006. An alternative bactericidal mechanism of action for lantibiotic peptides that target lipid II. Science, 313:1636-1637.

19. Smith, L., Hasper, H., Breukink, E., Novak, J., Čerkasov, J., Hillman, J. D., Orugunty, R. S. 2008. Elucidation of the antimicrobial mechanism of mutacin 1140. Biochemistry, 47:3308-3314.

20. van Heusden H E, de Kruijff B, Breukink E. 2002. Lipid II induces a transmembrane orientation of the pore-forming peptide lantibiotic nisin. Biochemistry, 41: 12171-12178.

21. Bonelli, R. R., Schneider, T., Sahl, H. G., Wiedemann, I. 2006. Insights into in vivo activities of lantibiotics from gallidermin and epidermin mode-of-action studies. Antimicrobial agents and chemotherapy, 50, 1449-1457.

22. Field, D., Connor, P. M., Cotter, P. D., Hill, C., Ross, R. P. 2008. The generation of nisin variants with enhanced activity against specific gram - positive pathogens. Molecular microbiology, 69, 218-230.

23. Rollema, H. S., Kuipers, O. P., Both, P., De Vos, W. M., Siezen, R. J. 1995. Improvement of solubility and stability of the antimicrobial peptide nisin by protein engineering. Applied and environmental microbiology, 61, 2873-2878.

24. Koopmans, T., Wood, T. M., 't Hart, P., Kleijn, L. H., Hendrickx, A. P., Willems, R. J., Martin, N. I. 2015. Semisynthetic lipopeptides derived from nisin display antibacterial activity and lipid II binding on par with that of the parent compound. Journal of the American Chemical Society, 137, 9382-9389.

25. Bierbaum, G., Szekat, C., Josten, M., Heidrich, C., Kempter, C., Jung, G., Sahl, H. G. 1996. Engineering of a novel thioether bridge and role of modified residues in the lantibiotic Pep5. Applied and environmental microbiology, 62, 385-392.

26. Ottenwälder, B. I. R. G. I. T., Kupke, T., Brecht, S., Gnau, V., Metzger, J., Jung, G., Götz, F. 1995. Isolation and characterization of genetically engineered gallidermin and epidermin analogs. Applied and environmental microbiology, 61, 3894-3903.

27. Chen, S., Wilson-Stanford, S., Cromwell, W., Hillman, J. D., Guerrero, A., Allen, C. A., Smith, L. 2013. Site-directed mutations in the lanthipeptide mutacin 1140. Applied and environmental microbiology, 79, 4015-4023.

28. Delves-Broughton, J., Blackburn, P., Evans, R. J., Hugenholtz, J. 1996. Applications of the bacteriocin, nisin. Antonie Van Leeuwenhoek, 69, 193-202.
29. Chan, W. C., Leyland, M., Clark, J., Dodd, H. M., Lian, L. Y., Gasson, M. J., Roberts, G. C. K. 1996. Structure - activity relationships in the peptide antibiotic nisin: antibacterial activity of fragments of nisin. FEBS letters, 390, 129-132.
30. Goldstein, B. P., Wei, J., Greenberg, K., Novick, R. 1998. Activity of nisin against Streptococcus pneumoniae, in vitro, and in a mouse infection model. The Journal of antimicrobial chemotherapy, 42, 277-278.
31. Ghobrial O, Derendorf H, Hillman J D. 2010 Pharmacokinetic and pharmacodynamic evaluation of the lantibiotic MU1140. Journal of pharmaceutical sciences, 99: 2521-2528.
32. Gross, E., and J. L. Morell. Peptide with alpha, beta unsaturated acids. In E. Scoffone (ed.), Peptides 1969. Elsevier/North-Holland Publishing Co., Amsterdam. 1971;356–360.
33. Rink, R., Wierenga, J., Kuipers, A., Kluskens, L. D., Driessen, A. J., Kuipers, O. P., Moll, G. N. 2007. Dissection and modulation of the four distinct activities of nisin by mutagenesis of rings A and B and by C-terminal truncation. Applied and environmental microbiology, 73, 5809-5816.
34. Kraaij, C., Breukink, E., Rollema, H. S., Siezen, R. J., Demel, R. A., Kruijff, B., Kuipers, O. P. 1997. Influence of charge differences in the C - terminal part of nisin on antimicrobial activity and signaling capacity. The FEBS Journal, 247, 114-120.
35. Geiger, C., Spieß, T., Korn, S. M., Kötter, P., Entian, K. D. 2017. Specificity of subtilin-mediated activation of histidine kinase SpaK. Applied and environmental microbiology, 83, e00781-17.
36. Cotter, P. D., Deegan, L. H., Lawton, E. M., Draper, L. A., O'connor, P. M., Hill, C., Ross, R. P. 2006. Complete alanine scanning of the two - component lantibiotic lacticin 3147: generating a blueprint for rational drug design. Molecular microbiology, 62, 735-747.
37. Caetano, T., Krawczyk, J. M., Mösker, E., Süssmuth, R. D., Mendo, S. 2011. Heterologous expression, biosynthesis, and mutagenesis of type II lantibiotics from Bacillus licheniformis in Escherichia coli. Chemistry & biology, 18, 90-100.
38. Escano, J., Stauffer, B., Brennan, J., Bullock, M., Smith, L. 2015. Biosynthesis and transport of the lantibiotic mutacin 1140 produced by Streptococcus mutans. Journal of bacteriology, 197, 1173-1184.
39. Lubelski J, Khusainov R, Kuipers OP. 2009. Directionality and coordination of dehydration and ring formation during biosynthesis of the lantibiotic nisin. J Biol Chem 284: 25962–72.
40. Lee, M. V., Ihnken, L. A. F., You, Y. O., McClerren, A. L., Donk, W. A. V. D., Kelleher, N. L. 2009. Distributive and directional behavior of lantibiotic synthetases revealed by high-resolution tandem mass spectrometry. Journal of the American Chemical Society, 131, 12258-12264.

41. Mierau I, Kleerebezem M. 2005. 10 years of the nisin-controlled gene expression system (NICE) in Lactococcus lactis. Applied microbiology and biotechnology, 68: 705-717.
42. Majchrzykiewicz, J. A., Lubelski, J., Moll, G. N., Kuipers, A., Bijlsma, J. J., Kuipers, O. P., Rink, R. 2010. Production of a class II two-component lantibiotic of Streptococcus pneumoniae using the class I nisin synthetic machinery and leader sequence. Antimicrobial agents and chemotherapy, 54, 1498-1505.
43. Escano, J., Stauffer, B., Brennan, J., Bullock, M., Smith, L. 2014. The leader peptide of mutacin 1140 has distinct structural components compared to related class I lantibiotics. Microbiologyopen, 3, 961-972.
44. Field, D., Begley, M., O'Connor, P. M., Daly, K. M., Hugenholtz, F., Cotter, P. D., Ross, R. P. 2012. Bioengineered nisin A derivatives with enhanced activity against both Gram positive and Gram negative pathogens. PLoS One, 7, e46884.
45. Kuipers, O. P., Rollema, H. S., Yap, W. M., Boot, H. J., Siezen, R. J., de Vos, W. M. 1992. Engineering dehydrated amino acid residues in the antimicrobial peptide nisin. Journal of Biological Chemistry, 267, 24340-24346.
46. Smith, L., Zachariah, C., Thirumoorthy, R., Rocca, J., Novák, J., Hillman, J. D., Edison, A. S. 2003. Structure and dynamics of the lantibiotic mutacin 1140. Biochemistry, 42, 10372-10384.
47 Breukink E, de Kruijff B. 2006. Lipid II as a target for antibiotics. Nature reviews Drug discovery, 5: 321-323.
48. Islam, M. R., Shioya, K., Nagao, J., Nishie, M., Jikuya, H., Zendo, T., Sonomoto, K. 2009. Evaluation of essential and variable residues of nukacin ISK - 1 by NNK scanning. Molecular microbiology, 72, 1438-1447.
49 Bomar, L., Brugger, S. D., Yost, B. H., Davies, S. S., Lemon, K. P. 2016. Corynebacterium accolens releases antipneumococcal free fatty acids from human nostril and skin surface triacylglycerols. MBio, 7:e01725-15.
50. Escano, J., Deng, P., Lu, S. E., Smith, L. 2016. Draft genome sequence of oral bacterium Streptococcus mutans JH1140. Genome announcements, 4, e00472-16.
51 . Xie, Z., T. Okinaga, F. Qi, Z. Zhang, J. Merritt. 2011. Cloning-independent and counterselectable markerless mutagenesis system in Streptococcus mutans. Appl. Environ. Microbiol. 77:8025–8033.
52. Li Y-H, Tang N, Aspiras MB, Lau PCY, Lee JH, Ellen RP, Cvitkovitch DG. 2002. A quorum-sensing signaling system essential for genetic competence in Streptococcus mutans is involved in biofilm formation. J Bacteriol 184:2699–2708.
53. Clinical and Laboratory Standards Institute. 2009. Methods for dilution antimicrobial susceptibility tests for bacteria that grow aerobically; approved standard—eighth edition. CLSI document M07-A8. Clinical and Laboratory Standards Institute, Wayne, PA.
54. Ellis, D., Gosai, J., Emrick, C., Heintz, R., Romans, L., Gordon, D., Smith, L. 2012. Occidiofungin's chemical stability and in vitro potency against Candida species. Antimicrobial agents and chemotherapy, 56:765-769.

55. Wilson-Stanford, S., Kalli, A., Håkansson, K., Kastrantas, J., Orugunty, R. S., Smith, L. 2009. Oxidation of lanthionines renders the lantibiotic nisin inactive. Applied and environmental microbiology, 75, 1381-1387.

A

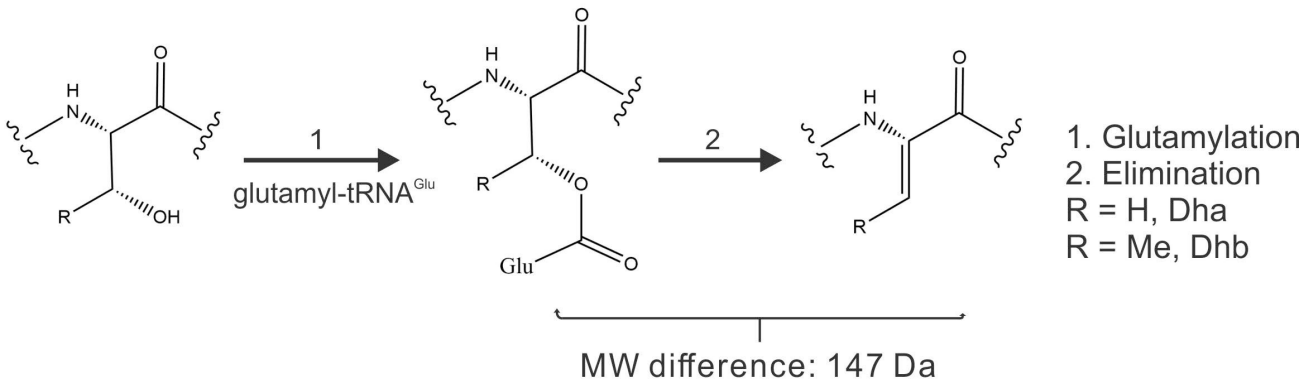

B

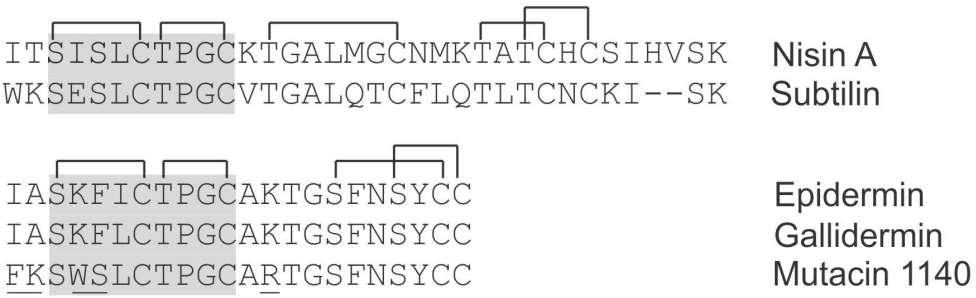

C